Proton Treatment Delivery Techniques

2

Xuanfeng Ding, Haibo Lin, Jiajian Shen, Wei Zou, Katja Langen, and Hsiao-Ming Lu

Contents

2.1 Introduction of Proton Treatment Delivery System 18
2.2 Treatment Delivery Techniques of Proton Therapy 20
2.2.1 Passive-Scattering 20
2.2.2 Pencil Beam Scanning 24
2.3 Imaging for Proton Beam Therapy 25
2.4 Intra-fractional Motion Management for Proton Therapy 28
2.5 Proton Beam Therapy Systems and Specifications 30
2.6 Quality Assurance (QA) 33
2.6.1 System QA 33
2.6.2 Patient-Specific QA (PSQA) 37
2.7 Future Developments 42
References 43

X. Ding
Beaumont Health, Royal Oak, MI, USA

H. Lin • W. Zou
University of Pennsylvania, Philadelphia, PA, USA

J. Shen
Mayo Clinic, Phoenix, AZ, USA

K. Langen
University of Maryland, Baltimore, MD, USA

H.-M. Lu (✉)
Massachusetts General Hospital, Boston, MA, USA
e-mail: HMLU@mgh.harvard.edu

N. Lee et al. (eds.), *Target Volume Delineation and Treatment Planning for Particle Therapy*, Practical Guides in Radiation Oncology,
https://doi.org/10.1007/978-3-319-42478-1_2

2.1 Introduction of Proton Treatment Delivery System

Proton therapy systems include three major components, the accelerator which raises the energy of the proton to a sufficient level, the energy selection and beam transportation system which modifies the proton energy, if necessary, and transports them from the accelerator to the treatment delivery system, and the treatment delivery system which modifies the proton beam characteristics for specific treatment needs. Currently, three types of accelerator, synchrotron, cyclotron, and synchrocyclotron, are commercially available, as discussed in the previous chapter. Protons generated from a cyclotron have a fixed energy, and energy reduction and selection systems are required, as shown in Fig. 2.1a. A synchrotron, on the other hand, can produce protons at any desired energy level. A synchrocyclotron is a special type of cyclotron that is typically used for a compact proton system. The beam transportation system (Fig. 2.1b), consisting of a sequence of dipole (bending and steering) magnets and quadrupole (focusing) magnets, delivers the proton beam from accelerator to treatment room through its vacuum beam pipeline. The beam switching from one treatment room to another is achieved by controlling the dipole deflector units along the beam transportation system.

The treatment delivery system is one of the main components of a proton therapy facility. It consists of several major subsystems: gantry, nozzle, snout, and patient positioning system in a treatment room. Proton beams are transported into a treatment room containing either fixed-beam lines or an isocentric gantry, as shown in Fig. 2.2.

A fixed-beam treatment room can have either one horizontal beamline (Fig. 2.2a) or the combination of a horizontal beamline and an angled beamline (e.g., 30° and

Fig. 2.1 Cyclotron and energy selection system (**a**) and a section of the beam transportation system (**b**) for a proton therapy facility (Courtesy of IBA, SA). Vacuum tube with multiple steering or bending magnets guide and focus the narrow proton beam to treatment rooms

90° for IBA inclined-beam gantry in Fig. 2.2c). The motivation of this design is to reduce the treatment room size and the overall cost. In the current stage, most fixed-beam and incline gantry rooms have been used for bilateral prostate cancer treatment as well as some cranial tumor with non-coplanar beam angles, e.g., vertex direction.

A gantry room provides either full 360° rotation (Fig. 2.2b) or limited rotations 0–220° (Fig. 2.2d) for the treatment. These gantry configurations are able to treat most of complicated cases which require different beam angles, e.g., the head and neck, lung, abdomen, etc. The standard full gantry is typically about 10 m in diameter with a total weight of up to 200 tons. A room with floor-to-ceiling height of about 20 m is required to accommodate such a structure and its base. Some compact gantries were designed with much smaller size and lighter weight around 100 tons.

The nozzle is the final element of the beam delivery system, which not only delivers the beam to the patient but also monitors the beam quality, alignment, and the dose delivery during treatment. There are two main types of nozzles: the nozzle that houses scattering components for passive-scattering (PS) delivery and the nozzle that houses components for pencil beam scanning (PBS) delivery.

- The PS nozzle contains first scatterers, range modulators, second scatterers, dose and field monitor chambers, patient-specific beam-shaping apertures, or other collimation components and compensators, as shown in Fig. 2.3a.

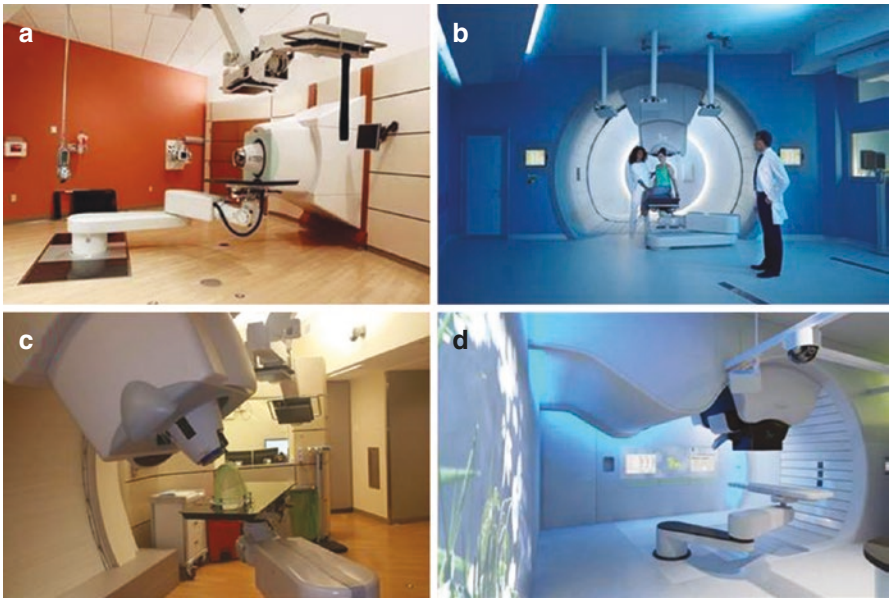

Fig. 2.2 Treatment rooms with different flexibilities of beam angles: (**a**) horizontal fixed-beam room, (**b**) 360° full gantry room, (**c**) inclined fixed-beam room (beam at 90° and 30° only), and (**d**) compact gantry (beam from 0° to 220°) (Courtesy of IBA, SA)

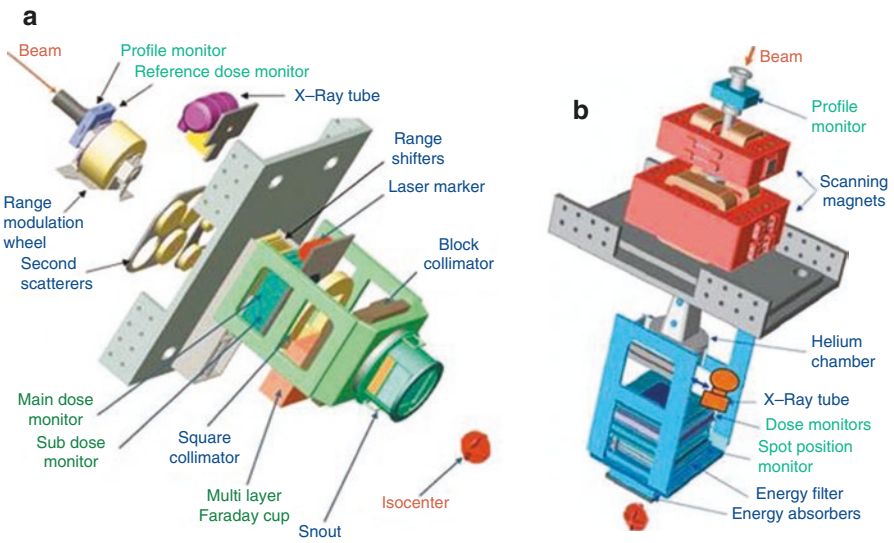

Fig. 2.3 Three-dimensional rendering of (**a**) the passive-scattering nozzle and (**b**) the scanning beam nozzle of the M.D. Anderson proton system (Hitachi Inc.) [1]

- The PBS nozzle contains the beam profile monitor, scanning magnets, dose and spot position monitor chambers, energy filter and range shifter (energy absorber), and possibly vacuum or Helium chambers on the beam path as well (Fig. 2.3b).

In addition to nozzles dedicated either for PS or PBS treatment delivery, some vendors provide nozzles with both scattering and scanning delivery capabilities, e.g., universal nozzle. However it can take a substantial amount of time to switch between different delivery modalities (e.g., IBA universal nozzle at the University of Pennsylvania).

2.2 Treatment Delivery Techniques of Proton Therapy

2.2.1 Passive-Scattering

Passive scattering is a conventional treatment technique in proton therapy. It utilizes the focused proton beam transported from the accelerator and scatters it through single or double scatterers to obtain a beam with large field size. In the proton beam scattering process, other components in the beam line will further modify the beam, for example, absorbers adjust the beam to the desired energy; modulator wheels or ridge filters modulate the beam to form a spread-out Bragg peak (SOBP) with a dose plateau. The scatterers, absorbers, modulator wheels, or ridge filters are usually installed in the treatment nozzle. At the end of the nozzle before the beam reaches patient, other devices such as apertures or MLC are inserted to the beam

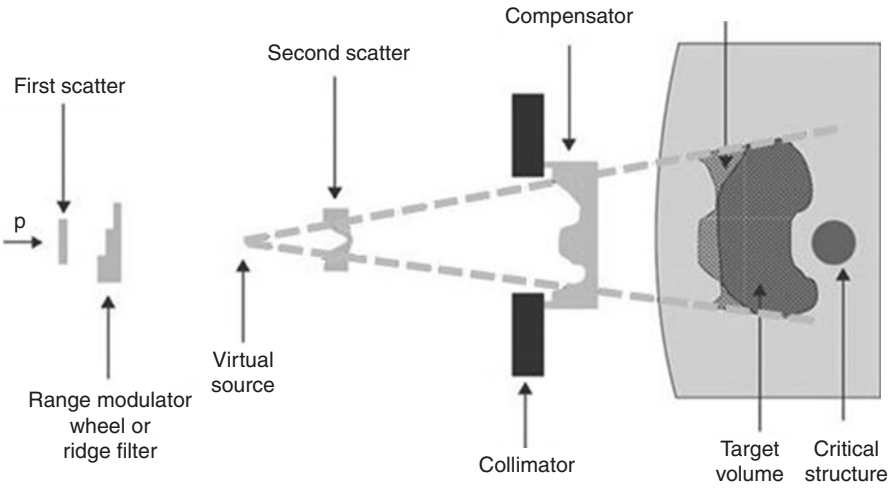

Fig. 2.4 Illustration of passive-scattering delivery technique [2]. Beam monitoring ionization chambers are not shown

line to collimate the beam to the shape of the treatment target. A compensator with varying thickness profile is also used to shape the distal penetration of the beam to the distal shape of the treatment target (Fig. 2.4).

2.2.1.1 Single Scattering

Single-scattering technique utilizes one scatterer in the beam line to scatter the focused proton beam into a large field. The scatterer is usually made from high atomic number foil such as lead. The proton beam passing through the single scatterer is laterally dispersed. The resulting proton field can be of nonuniform Gaussian-shaped intensity across the field. However, the central portion of the beam can be sufficiently uniform for treatment of small targets such as eye lesions. A single-scattering system generally produces sharper lateral beam penumbra than double-scattering systems and is therefore more often used for eye or brain tumor treatments.

2.2.1.2 Double Scattering

In double-scattering system, downstream from a first scatterer foil that scatters the proton beam into a Gaussian-shaped intensity field, a second scatterer is used to flatten the transverse intensity across the field. The second scatter is usually made of high Z material such as lead with a compensating thin layer of low Z material such as polycarbonate. The shape of the high Z material is close to a Gaussian with the thickest portion at the center. The double-scattering system can achieve uniform field intensity at a large field size up to 40 cm in diameter.

In a passive-scattering system, the delivery of a uniform dose across the depth of the target is usually achieved through the construction of SOBP. The SOBP is made of a series of intensity and energy-modulated pristine Bragg peaks. The system

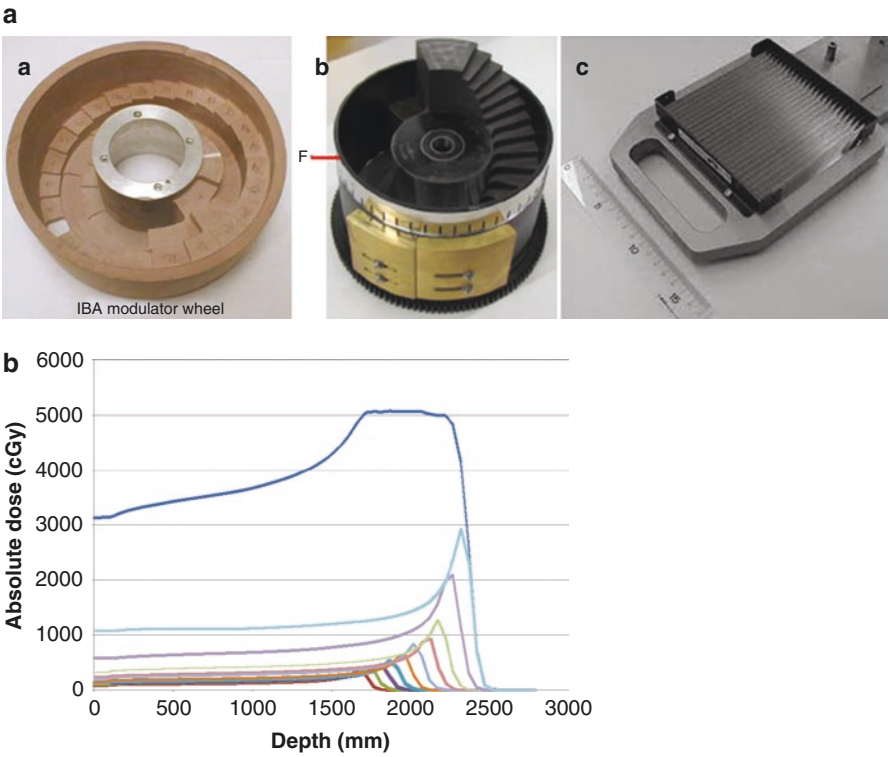

Fig. 2.5 (**a**) Devices for SOBP construction: *a* IBA three-track modulator wheel, *b* Mevion single-track modulator wheel, *c* HIBMC ridge filter [3]. (**b**) Generation of SOBP using passive-scattering technique. *Red line graph* shows the spread-out Bragg peak (SOBP) peak. There are ten lines of pristine Bragg peak which indicates the different proton energies and dose depositions after going through the modulation wheel in order to treat a target uniformly using the SOBP (*dark blue line*). The sum of the individual line equals to the *dark blue line*

achieves this through a range modulator wheel or ridge filter (Fig. 2.5a, b). The modulator wheels are made of a series of steps from low Z material with varying step heights and widths. As the wheel rotates at a constant speed, the proton beam passes the steps in sequence so that the beam energy is reduced to produce the group of Bragg peaks with the required proton energies and intensities for the construction of SOBP. The ridge filter modulates the proton beam through a series of stationary localized ridge-shaped bars. The ridge profile, taking into the account of beam scattering and energy reduction, is designed with the height and the spread to construct the desired SOBP [3].

2.2.1.3 Uniform Scanning

Uniform scanning utilizes a first scatterer to scatter the beam to a slightly larger beam spot, typically several centimeters. The scanning magnets downstream in the beam line have two perpendicular sets of magnets to sweep the proton spot, with a

fixed frequency (e.g., 30 Hz) across the transverse plane over a rectangular or circular (so-called wobbling) area that covers the maximum projected dimension of the target volume. Longitudinally, the target volume is covered layer by layer, usually from deep to shallow, by changing the beam energy. In one particular implementation, the energy change is achieved by building a special track on the modulator wheel but with equal length steps and equal thickness difference between subsequent steps (e.g., the outmost track in Fig. 2.5). During treatment, the modulator wheel rotates in a "step and shoot" manner to produce the desired beam energy for each corresponding scanning layer. Thin range shifters may also be used upstream to reduce further the layer spacing down to a millimeter. The beam intensity stays uniform within each layer, but relative intensities between layers are adjusted in order to produce a SOBP depth dose distribution with a dose plateau when measured in water. The second scatterer is not needed, but patient-specific field apertures/MLC and compensators are used as in passive scattering.

In both the passive-scattering and uniform-scanning treatment delivery mode, apertures are custom cut from brass (or cerroband). Brass has a high proton stopping power ratio of 5.6 to water. Some proton beam systems have utilized MLC in place of apertures. MLC can save the effort of block cutting and block mounting; however, it often has a restricted field size. The compensators are milled from a block of PMMA or wax. PMMA compensators are more rigid and transparent but non-recyclable as opposed to wax. The thickness profile of the compensator is patient beam specific and is usually calculated in the patient treatment plan and exported to the milling machine (Fig. 2.6).

Current treatment planning systems (TPS) do not usually support the calculation of beam MU values for passive-scattering treatments. The MUs are determined either from direct measurements with ion chambers in water or water equivalent materials or from analytic models with parameters derived from measured data [4]. A major disadvantage of scattering systems are that the use of compensators only conforms the dose distribution to the distal shape of the target but not the proximal side (see Fig. 2.4). It does not provide the capability to actively spare the organ at risk on the proximal side, although such dose spill can sometimes be mitigated by using multiple beam angles.

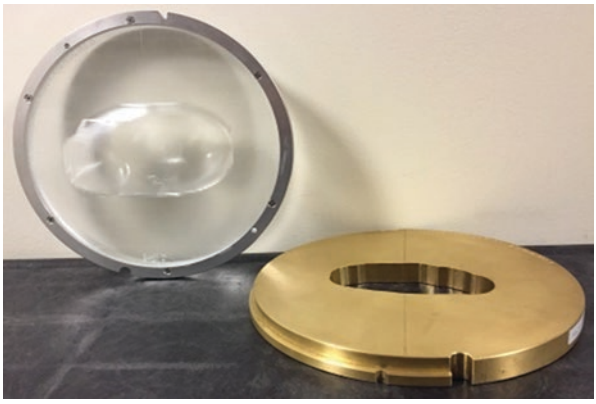

Fig. 2.6 Patient beam-specific brass aperture and PMMA compensator

The use of scatterers in the beam line results in a larger virtual source size and therefore increases the penumbra substantially. In addition, penumbra increases with the depth of penetration. During treatment, the apertures should be brought to as close to the patient as possible to reduce penumbra. The penumbra may also be slightly reduced by having the aperture cut divergently through its thickness, although such improvement is very small for systems with large SAD values (>200 cm).

2.2.2 Pencil Beam Scanning

The pencil beam scanning (PBS) technique was first introduced for patient treatment a couple of decades ago, and the technique has gone through a rapid expansion and development in the last decade. PBS is becoming the new standard technology in proton therapy, and for new centers PBS is often the only treatment modality.

In pencil beam scanning systems, two pairs of orthogonal dipole magnets (scanning magnets) are used to steer protons laterally (Fig. 2.7).

The scanning magnets sequentially direct a small size pencil beam to predetermined positions with desired intensity, i.e., the number of protons. The dose to the entire tumor is the superposition of each individual small size pencil beams. The PBS system is very complex because it requires a very fast and reliable control with adequate risk mitigation measures [5].

Proton pencil beam scanning technology naturally provides intensity-modulated proton therapy (IMPT) technique by varying the location of each pencil beam and the number of protons delivered to it. Its intensity modulation in the lateral direction is similar to IMRT. However, it also provides modulations in depth by varying proton energies, which IMRT cannot provide. As a result, PBS is capable of true 3D dose painting [6]. With the typical pencil beam size of a few mm, PBS can deliver highly conformal dose to any arbitrary shape. The IMPT technique vastly increases the proton applications in radiation therapy.

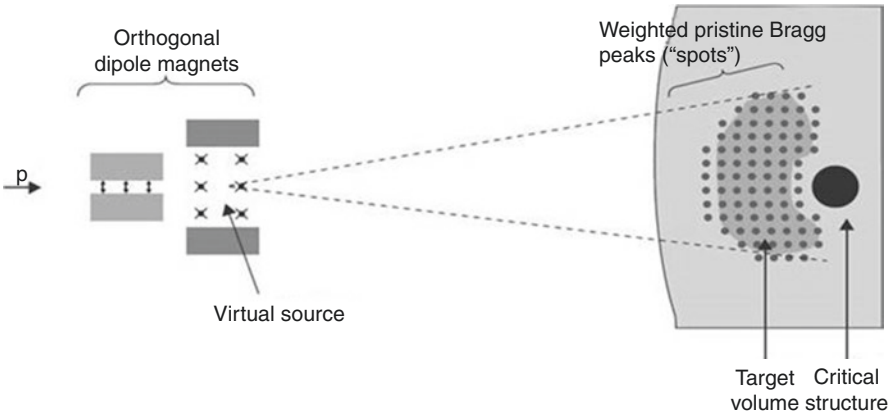

Fig. 2.7 A schematic representation of a scanning proton beam delivery system [2]

The delivery of pencil beam spots can be discrete or continuous. In continuous scanning, the beam is not turned off between spots, while in discrete spot scanning, it is completely turned off. Discrete spot scanning could avoid the transient dose uncertainties when beam moves to the next spot. However, the beam delivery is slowed due to the dead time (~several milliseconds) between spots. Although most of the current proton systems use discrete spot scanning, continuous scanning is being implemented in future systems by some manufactures.

Pencil beam scanning treatments generally do not need apertures and compensators as in passive scattering and uniform scanning. However, apertures may still be used to sharpen lateral beam penumbra, when the pencil beam spot size is too large to produce the desired dose gradient between the target volume and the organs nearby [7].

There are currently two main approaches to PBS treatment: single field optimization (SFO) technique, where each individual field uniformly covers a target, and multi-field optimization (MFO) technique, where each individual field only partially covers a target, but uniform target coverage is provided by the combination of all the fields included in the optimization. SFO and MFO are also regarded as SFUD and IMPT, respectively, in ICRU78. This book chapter uses SFUD and IMPT definition for consistency. The details of these optimization techniques and standards will be discussed in the next chapter.

Compared to passive scattering, pencil beam scanning has the following major advantages:

- Delivers 3D conformal dose to tumor in a single beam: distally, proximally and laterally (refer to treatment planning section).
- Reduces target dose heterogeneity due to presence of severe tissue heterogeneity, for example, in the treatment of head and neck cancers.
- Neutron production in air is significantly reduced due to the absence of beam-modifying hardware in the beam line.
- Eliminates time and resources required for the use of apertures and compensators.

Since each PBS beam is composed of thousands of individual spots, the final accuracy of the dose delivered to patient relies on how accurately each spot is delivered. The typical parameters that affect the dose accuracy are the spot position, spot shape, and the number of protons of each spot. For the scanning beam, it is very important to have a reliable and rapid-response control system that could deliver each spot to the desired position with the correct number of protons. Physicists design various quality assurance (QA) procedures to validate the system performance and patient-specific treatment delivery.

2.3 Imaging for Proton Beam Therapy

A variety of patient-specific imaging techniques are routinely used or still under development for planning, image guidance, or verification of proton treatment, which are summarized in Table 2.1. All the imaging techniques can be simply

Table 2.1 Summary of imaging techniques for proton therapy

Type of imaging	Application	Routine practice	Advantage	Challenges
CT	Anatomic structure delineation; dose and range calculation	Yes	High resolution; high bone-tissue contrast; anatomical imaging; fast acquisition time	Requires proton stopping power calibration; uncertainties due to calibration and CT artifacts translate to the proton beam range uncertainties
Dual-energy CT	Tissue decomposition	No	Increase the accuracy of the proton range calculation	Theoretical improvements in range predictions with DECT data in the order of 0.1–2.1% were observed [9]
MRI	Anatomic structure delineation	Yes	High spatial resolution and soft tissue contrast	Possible geometric distortion; direct use for dose calculation still under investigation
PET (for PET/CT)	Target volume delineation and identification	Yes	High sensitivity	Limited anatomic resolution and need to combine with CT
CT on-rails	Patient positioning; treatment verification	Yes	High resolution; fast acquisition time; allows adaptive planning and treatment	Require extra space in the treatment room; increase patient in-room time; unable to assess intra-fractional motion
Orthogonal kV planar imaging	2D patient positioning	Yes	High image quality especially for bone-tissue contrast	Low soft tissue contrast
CBCT	3D patient positioning; treatment verification	Yes	High spatial resolution of soft tissue	Poor image quality compared to CT, potential value for dose calculation and adaptive therapy under investigation
Optical imaging	Patient surface tracking and positioning	Yes	Fast, high sensitivity and real time acquisition; no radiation dose; large field of view; ideal for superficial target	No visualization of internal anatomy and relies on surrogates rather than target itself; skin needs to be visible and may have clearance issue
PET (treatment activated)	3D verification of treatment delivery	Only at limited institutions	In vivo verification of treatment	Require short time delay between treatment and imaging; reduced signals due to limitations of the imaging protocol (e.g., biological washout et al.)

Table 2.1 (continued)

Type of imaging	Application	Routine practice	Advantage	Challenges
Prompt gamma	Verification of proton ranges	No	In vivo verification of treatment; no biological washout effect	Require bulky equipment for signal collimation and detection. Clinical value remain to be demonstrated
Proton radiography and proton CT	Planning and treatment verification	No	Direct measurement of proton stopping power	Require high proton energy sufficient to penetrate the patient; limited spatial resolution due to multiple coulomb scattering

divided into three groups based on their purposes of applications. The first group including CT, MRI, and PET/CT is mainly used for structure delineation and dose calculation, which is very similar to photon/electron therapy. Since CT data does not provide directly proton stopping power ratio (SPR) required for proton dose calculation, a calibration procedure is required to establish the relationship between CT HU values and proton SPR. However, uncertainties in the HU to SPR calibration exist, and these uncertainties eventually translate to range uncertainties that have to be carefully accounted for during the planning stage [8]. Dual-energy CT improves the SPR production and has the potential to reduce the range uncertainties associated with HU to SPR calibration [9, 10]. However, more studies and evaluations are needed for future implementation in routine clinic. The second group is mainly used for patient alignment, verification of the treatment position before each treatment, and adaptive planning. It includes techniques such as orthogonal kV, CBCT, CT on rails, body surface imaging, etc. The third group includes particle therapy unique imaging techniques such as proton radiography, proton CT [11], treatment-activated PET imaging [12], or prompt gamma [13] imaging, many of which are in the process of being adopted or under development for the purpose of range and dose verification. Since the anatomical and physiological variations have greater impact on the proton dosimetry compared to their impact on the photon dosimetry, imaging may be frequently repeated during the proton treatment course for monitoring and validating the treatment.

Successful proton treatment delivery requires reproducible patient positioning during daily treatment. IGRT is essential for patient positioning and placement of devices used for treatment such as immobilization devices. Immobilization devices in the beam path should be considered consistently through simulation, planning, and treatment in terms of their locations and physical properties.

- Devices intersecting beam paths during treatment should be homogeneous, indexed, and included in the proton dose calculation during the planning stage; devices present during CT simulation, but not during treatment, should be excluded from the body contour for proton dose calculation. Couch overlay should be utilized consistently with what is planned.

- Any HU override for devices and artifacts during the planning stage should be carefully evaluated on a case by case basis. Inappropriate override of HU can lead to significant dose errors.
- Immobilization devices should be indexed to the treatment couch top when they are positioned in the treatment area or whenever possible.
- Partial beam blocking by any devices (couch, bolus et al.) is difficult to reproduce and should be avoided (e.g., large-angle posterior oblique field passing through the couch edge).
- Positions of range shifter and bolus should be minimized and consistent with those in planning. Air gaps between device and patient should be confirmed routinely. Air gaps between the range shifter (or bolus) and the patient should be kept the same to maintain the spot profile. The couch top is generally made of uniform low-density material, but some institutions have purposely used thicker substitutes as range shifters for spot-scanning treatment.

2.4 Intra-fractional Motion Management for Proton Therapy

The management of intra-fractional target motion during proton therapy depends on the specific proton treatment technique.

- Passively scattered proton beams are more akin to 3D photon treatment techniques in the sense that the whole treatment field is delivered simultaneously. A modified ITV concept ensuring that the target is covered during all motion phases may be used to provide sufficient target coverage. The variations in WET due to intra-fractional motion may be accounted for in the compensator design. Kang et al. described the treatment planning strategies for mobile lung tumors treated by passively scattered proton beams. A 4D CT scan is used to derive the internal gross tumor volume (IGTV). For planning purposes the average CT scan is used; however, the IGTV volume density is overwritten with uniform density value of 100HU [14] or established based on the average ICTV HU values for each case.
- The use of pencil beam scanning presents a different challenge in the sense that it is more akin to IMRT because only subsections of the target volume are treated at any given time. The dynamics of the treatment delivery and a moving target can lead to interplay effects that need to be assessed and managed.

For either delivery technique, it is beneficial to restrict the amount of motion during beam delivery. Abdominal compression as well as gating have been successfully employed by some groups during proton therapy treatments [15, 16].

On the other hand, it is unlikely that a target in motion can be managed to a degree that it can be treated as stationary.

- For unmanaged or a given residual motion, it is of interest to assess the dosimetric impact of the target motion. This simulation requires accurate knowledge and synchronization of the proton delivery dynamics and moving patient anatomy. A number of research groups have developed in-house simulators to assess the dosimetric impact of motion [15, 17]. The dosimetric impact depends on the timing of the treatment with respect to the breathing phases. While researchers demonstrated that the dosimetric effect of a single fraction delivery can be concerning, it has also been demonstrated that the dosimetric effect averages out quickly after the delivery of several fractions [17, 18]. However, the effect is treatment site and patient specific.
- The cumulative dosimetric effect of target motion after the completion of a fractionated course of treatment is of interest has been investigated. Using a realistic interplay simulator, Li et al. showed that after the delivery of a regular fractionated treatment, the cumulative dose distribution approaches that of the 4D dose distribution [17]. The latter is obtained by recalculating the nominal plan into each 4DCT phase and accumulating the dose distributions from the individual phases onto the nominal treatment planning CT using deformable image registration. The calculation of the 4D dose does not require an interplay simulator and is relatively easy to implement in commercial treatment planning systems.
- The magnitude of the dosimetric effect will be a function of plan and patient parameters.
  - Grassberger et al. reported that the dosimetric effect of motion is reduced with increasing spot size [18]. While the spot size is typically not variable for a given scanning nozzle, it can be manipulated by the use of external range shifters and by varying the air gap between the range shifter and the patient's skin.
  - Grassberger et al. reported an increase of the motion effect with motion magnitude.
  - Li et al. reported that motion effects may be enhanced if the CTV is small with respect to motion magnitude [17].
  - With respect to dose modulation, Dowell et al. report that the amount of dose modulation for targets that moved less than 20 mm had no significant effect [19].
  - Zeng et al. [20, 21] report that for single-beam PBS treatments of mediastinal lymphomas, the cumulative dosimetric degradation (D98%) was less than 2% and up to 5% for single factions. Actual breathing phases as measured at time of 4DCT were used for this simulation.
- Other groups have investigated modified delivery techniques to make spot-scanning plans more robust against intra-fractional motion.
  - Repaint the target volume, i.e., each spot location is revisited by the scanning beam multiple times which is a widely discussed option. In general two techniques have been developed. In the first technique, termed layered repainting, each energy layer is repainted several times until all MUs are delivered. This is repeated for each subsequent layer. In the second

technique, termed volumetric repainting, the complete target is painted multiple times [22]. A disadvantage of the techniques is that each volumetric repaint requires each energy layer to be revisited. This will increase the treatment time and hampers the use of this technique for systems that have a longer layer switching times. The latter technique is, however, relatively simple to implement by increasing the fractionations by multiples of n. Each repainting technique however has to account for machine delivery limitations such as the minimum MU per spot limit. A spot which is planned to deliver MUs close to the minimum MU cannot be repainted with either method. To manage these machine limitations various refined repainting techniques have been reported.

- In a recent publication Li et al. investigated a spot sequence optimization technique to increase the plan's robustness against motion. The spot map delivery was altered to increase the distance between subsequent spot deliveries [23]. This sparser delivery sequence resulted in more robust plans.
- Motion robust treatment planning techniques have also been developed. Yu et al. reported the use of 4D robustness optimization in conjunction with beam angle optimization [24]. For 4D optimization, plans were robustly optimized on multiple 4D CT phases. In addition beam angles were evaluated for changes in WET with respiration and angles with minimal changes in WET were selected for treatment planning.

To summarize, the dosimetric impact of motion on proton therapy treatments has been studied widely for proton plans. While no single solution has emerged, multiple techniques have been reported to be useful for target motion management during proton therapy.

2.5 Proton Beam Therapy Systems and Specifications

In recent decades, due to the increasing demands for proton beam therapy, many manufacturers have started to join the market. So far, there are many proton system configurations, techniques, and combinations developed to fit the needs of various institutions. In the meanwhile, proton beam therapy technology has continued to evolve rapidly. The goal of this section is to summarize the clinical systems currently available commercially to provide the reader with a brief account of the important machine parameters and characteristics which could have a significant clinical impact on treatment and protocol development. The clinical parameters quoted in Table 2.2 are based on proton centers actively treating patients as of May 2016 (Tables 2.3 and 2.4).

Table 2.2 The summary of proton system specifications in clinical operation

Manufacture	Model	Accelerator type	Clinical beam ranges	Treatment room options	IGRT system	Treatment modality
IBA	ProteusPlus	Cyclotron	32.0 g/cm^2; 4.1 g/cm^2	Fix beam line, inclined gantry, and full gantry	2D orthogonal imaging; CBCT; CT on rail	PBS[a], US[b], DS[b], SS[b]
IBA	ProteusONE	Superconducting synchrocyclotron	32.0 g/cm^2; 4.1 g/cm^2	220° compact single-room gantry	Stereotactic imaging; CBCT	PBS only
VARIAN	ProBeam	Superconducting cyclotron	36.0 g/cm^2; 4.1 g/cm^2	Fix beam line and full gantry	2-D orthogonal imaging; CBCT	PBS only
HITACHI	ProBEAT	Synchrotron	32.4 g/cm^2; 4.0 g/cm^2	Fix beam line, 180° gantry, and full gantry	2-D orthogonal imaging; CT on rail	PBS, US, DS, SS
Mevion	S250	Superconducting synchrocyclotron	32.0 g/cm^2; 5.0 g/cm^2	180° compact single-room gantry	2-D orthogonal imaging; CT on rail (planned)	DS
Sumitomo	P235	Cyclotron	32.0 g/cm^2; 3.8 g/cm^2	Full gantry	2D orthogonal imaging; CBCT (planned)	US, DS, PBS

[a]*PBS* Pencil Beam Scanning treatment delivery technique
[b]*DS* Double-scattering treatment delivery technique; *US* Universal-scanning treatment delivery technique; *SS* Single-scattering treatment delivery technique

Table 2.3 Pencil Beam Scanning clinical parameters (spot scanning)

Parameters	Clinical significance	Most common values
Maximum field size	The maximum lateral dimension of the target that can be treated without using multi-iso fields	From 20 × 24 cm^2 to 30 × 40 cm^2
Energy layer switch time (ELST)	A major factor of spot-scanning beam delivery efficiency	Cyclotron <1 s synchrotron 1 ~ 2 s
Spot switch time	A minor factor of spot-scanning beam delivery efficiency	2–10 ms
Spot size (1 sigma in air)	The lateral penumbra of the dose distribution	2.2–4.4 mm at 32 g/cm
Spot symmetry	The quality and consistency of the proton beam for all gantry angles and energies	10%
Spot position accuracy	The quality and consistency of the proton beam position accuracy for all gantry angles and energies	1 mm
Length of time for irradiating a 1 L target to a uniform dose of 2 Gy	Overall estimation of the treatment delivery efficiency of a proton system	30–120 s
Remote air gap tuner	Capable of adjusting air gap between range shifter to patient' skin in order to optimize the spot size for the treatment	Continuous/fixed/ discrete position
Room switch time (RST)	The operation efficiency of a multiroom proton therapy center	10–60 s

Table 2.4 Passive-scattering clinical parameters

Parameters	Clinical significance	Most common values
Maximum field size	The maximum lateral dimension of the target that can be treated without using multi-iso fields	15 cm; 25 cm diameter (DS); 30 × 40 cm (US)
Dose rate	Major factor of passive-scattering beam delivery efficiency	2 Gy/min; 1 Gy/min
Number of modulation wheels and options	Number of combinations of SOBP and beam range	14 modulator wheels, 24 options (Mevion) 3 modulator wheels and 8 options (IBA)
Modulation wheel warm up time before irradiation	A minor factor of passive-scattering beam delivery efficiency	30–60s
Collimation system	Manual or auto configuration of the beam lateral shape	MLC/brass aperture
Room switch time (RST)	The operation efficiency of a multiroom proton therapy center	10–60s

2.6 Quality Assurance (QA)

2.6.1 System QA

A detailed and comprehensive physics QA protocol is needed to ensure system performance and patient safety. Table 2.5 summarizes the major mechanical and dosimetry-related QA items and procedures of most common proton therapy systems. It includes the daily, weekly, monthly, and annual QA items followed by a

Table 2.5 QA tasks and procedures for proton therapy systems

Items	Frequency	Description	Measurement devices
	Beam dosimetry parameters for PBS		
Output	Daily; monthly; annually	*Purpose*: verify monitor chambers' integrity and reliability, as well as beam characteristics and fluence consistency *Method*: measure the beam output at the center of modulation (the center of the SOBP) using a broad uniform field. Criteria: 2%	Cylindrical farmer type; parallel plate ionization chamber (PPIC) Fig. 2.8a
Range	Daily; monthly; annually	*Purpose*: verify the stability of the machine for delivering predetermined beam energies *Method*: range of individual spots and a uniform large field. Commonly used phantoms with varying thickness, e.g., a custom-made wedge phantom Criteria: 1 mm	PPIC with scanning water tank; multilayer ionization chamber (MLIC) Fig. 2.8b
Dose flatness and symmetry	Daily; monthly, annually	*Purpose*: verify beam stability and reproducibility of the beam optics at nominal and all gantry angles *Method*: measure 2D dose distributions and compare with commissioning data in TPS Criteria: 1%	Scintillator/CCD camera system; ion chamber array; film
Distal dose falloff	Monthly; annually	*Purpose*: verify the constancy of beam energy spread which could affect the integral depth dose distributions (IDDD) *Method*: measure depth dose distributions Criteria: 1 mm	PPIC with scanning water tank; multilayer ionization chamber (MLIC) (may be combined with range check procedure)
Spot profile	Daily; monthly; annually	*Purpose*: verify spot profile consistency. *Method*: measure individual spot profile Criteria: 10% (1-sigma)	Film, ion chamber array, strip chambers, or scintillator/CCD detecting system. (Fig. 2.8c)

(continued)

Table 2.5 (continued)

Items	Frequency	Description	Measurement devices
Spot position	Daily; monthly; annually	*Purpose*: verify spot position accuracy *Methods*: deliver several sets of spot pattern and verify their positions Criteria: 1 mm	Film, ion chamber array (Fig. 2.8d), strip chambers, or scintillator/CCD detecting system (can be combined with spot profile procedure)
Pencil beam depth dose distribution	Annually	*Purpose*: verify integral dose of the pencil beam at different depths *Method*: measure depth dose using a Bragg peak ion chamber in a water tank equipped with scanning capabilities	Bragg peak ion chamber
Spot angular-spatial distribution and lateral dose profiles	Annually	*Purpose*: verify spot dose lateral profiles and at different depths *Methods*: measure individual spot profile Criteria: 20% (spot symmetry)	Film, small volume ion chambers, scintillator/CCD camera system
Inverse square correction test	Annually	*Purpose*: verify the distance of the point of measurement for broad fields from the "effective source" position *Method*: measure dose with an ionization chamber at different distances relative to isocenter and compare it with the predicted dose using the inverse square correction factor	2D ion chamber array
Monitor chamber linearity, reproducibility, and min/max checks	Annually	*Purpose*: verify linearity, reproducibility, minimum and maximum dose criteria of the monitor chambers for PBS delivery *Method*: measure dose by decreasing/increasing the intensity of spots to the tolerance levels Criteria: 1%	PPIC
	Patient setup verification		
Laser	Daily	*Purpose*: verify the laser-projected position relative to isocenter of the imaging system *Method*: position a phantom with fiducials at isocenter using the imaging system and verify the laser projections on the phantom Criteria: 1 mm	IGRT phantom (Fig. 2.8f)

Table 2.5 (continued)

Items	Frequency	Description	Measurement devices
IGRT system	Daily; monthly	*Purpose*: verify imaging system vs. radiation isocenter, as well as imaging quality *Method*: position IGRT phantom at isocenter using the imaging system and deliver proton beam at center of the field Criteria: 1 mm	IGRT phantom (combined with laser check procedure)
Communication and interface	Daily	*Purpose*: verify the interface between delivery and IGRT system and record and verification system *Method*: load a plan, acquire images, deliver treatment beams, and send records back to record and verification system. Check if all images and delivered dose are recorded	The procedure should be tested in treatment mode during one of daily QA testing items
Safety	Daily	Audiovisual monitor; visual monitor; beam-on indicator; X-ray on indicator; search/clear button; beam pause button; emergency beam stop button, monitor units interlocks; collision interlocks; radiation monitor system (neutron or X-ray); door interlock	N/A
Emergency stop	Monthly	*Purpose*: verify the emergency-stop buttons stop not only the mechanical movements but also the particle and/or the X-ray radiation	N/A
Mechanical systems			
Gantry angle vs. gantry angle indicators	Weekly	*Purpose*: verify the accuracy of the gantry angle as indicated on the gantry angle indicators or digital readout Criteria: 1°	Digital level
Snout extension	Weekly	*Purpose*: verify the mechanical accuracy of the snout positions with respect to the treatment plan Criteria: 1 mm	Meter stick
Collision sensors	Weekly	*Purpose*: check nozzle and imaging component collision sensors functionality	N/A
Couch positional	Weekly	*Purpose*: verify the accuracy of couch position with respect to treatment plan; normally 6° of freedom Criteria: 1 mm	Meter stick and digital level

(continued)

Table 2.5 (continued)

Items	Frequency	Description	Measurement devices
Gantry radiation Isocentricity	Monthly; annually	*Purpose*: verify the radiation isocenter accuracy with respect to the gantry angles *Method*: gantry star shot technique for central beam axis Criteria: 1 mm	Film Fig. 2.8h; XRV-100 Fig. 2.8f
Couch Isocentricity	Monthly; annually	*Purpose*: verify the radiation isocenter accuracy with respect to the couch rotations *Method*: couch star shot technique for central beam axis Criteria: 1 mm	Film
Additional QA items for passive-scattering systems			
SOBP width	Monthly; annually	*Purpose*: verify beam extraction and intensity that synchronized with the rotation of the modulator wheel in order to produce flat SOBPs *Method*: measure depth dose distributions for specified SOBP fields covering all options, that is, the use of the all beam-modifying components for SOBP construction Criteria: 1 mm	PPC with scanning water tank system; multilayer ionization chamber (MLIC) (can be combined with range check procedure)
Multi-leaf collimator	Monthly; annually	*Purpose*: alignments; leaf position; activation; interlock functionality	Survey meters; film
MLC leakage	Monthly; annually	*Purpose*: verify the requirements for the leakage dose from intraleaf, interleaf, leaf-end, leaf banks, and other MLC components *Method*: use the highest proton energy to check the leakage	Film

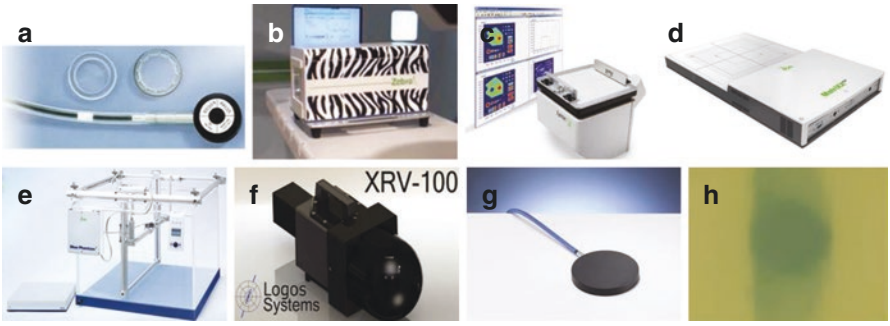

Fig. 2.8 Dosimetry equipments. (**a**) Parallel plate ion chamber: PPC05. (**b**) Multilayer ionization chamber: Zebra (IBA, Belgium). (**c**) Scintillator/CCD camera detector: Lynx (IBA, Belgium). (**d**) 2D ion chamber array: MatriXX (IBA, Belgium). (**e**) Water tank: Blue phantom 2 (IBA, Belgium). (**f**) IGRT phantom for PBS QA: XRV-100 (Logos Systems International, Scotts Valley, CA). (**g**) Bragg Peak Chamber: PTW (Freiburg GmbH). (**h**) Radiochromic films (Ashland, NJ)

brief description of the procedure and measurement devices required. Detailed IGRT QA procedures are not included here, since IGRT systems for proton therapy are in rapid transition, for example, toward volumetric imaging. CBCT for proton treatment has just been implemented at the University of Pennsylvania in 2015, and several centers have started using CT on rails recently. For 2D orthogonal imaging systems, interested readers may consult corresponding sections in AAPM task force report 142 (TG142) on image guidance in external beam therapy.

2.6.2 Patient-Specific QA (PSQA)

Patient-specific quality assurance (PSQA) has been one of the most important programs in radiation therapy workflows to ensure the accuracy of dose delivery for each treatment plan prior to the patient's treatment. Similar to clinical practice in QA procedures for intensity-modulated radiation therapy (IMRT), PSQA for proton therapy includes (1) absolute dose verification and (2) dose distribution verification. One major difference between IMRT and proton therapy is that the latter uses much fewer fields for each treatment fraction. In many cases, a single treatment field is sufficient to produce the satisfactory fractional dose distribution. Even in the case of IMPT multi-field optimizations for pencil beam scanning, the number of fields required is usually two to four, compared to IMRT where most treatments use five or more. As a result, PSQA for proton treatment has been conducted for each field, even in the case of IMPT, rather than for the composite dose from all fields as in the case of IMRT QA. This also results from the lack of reliable and efficient techniques for measuring three-dimensional dose distributions. Such QA measurement techniques, e.g., 3D gel dosimetry, are still not feasible for routine clinical practice due to various limitations. Overall, given the ongoing development of new treatment delivery, planning, and measurement techniques, PSQA for proton beam therapy is in the stage of rapid evolution and no gold standard exists currently for procedures and guidelines. The purpose of this section is therefore limited to providing a general idea about the most common PSQA procedures and dosimetry tools used at different institutions.

2.6.2.1 PSQA for Pencil Beam Scanning

As mentioned above, two types of optimization techniques are used for planning PBS treatment, SFUD, and IMPT. Treatment fields obtained from both techniques have modulated beam energies and intensities and generally do not produce homogeneous dose distributions in a phantom, creating challenges for measurements, although understandably substantially more so for IMPT than SFUD fields.

SFUD QA

SFUD is often used where the target is simple, and no critical organs at risk (OARs) are present along the beam path such as prostate cancer. A very comprehensive SFUD PSQA procedure based on prostate planning has been published by Zhu et al. [25]. The procedure includes three parts, (1) point dose verification, (2) central axis depth dose verification, and (3) relative 2D dose measurements, as listed in Table 2.6.

Table 2.6 An example of PSQA components for SFUD fields

Items	Procedure	Dosimetry device
Point dose verification	*Purpose*: (1) an end-to-end test of data transfer integrity from the TPS to the scanning beam accelerator control system (ACS); (2) verify the beam steering magnets are working properly for different gantry angles; (3) uploading of the required bending magnet field strengths *Methods*: measure point dose in the mid-SOBP position	MatriXX; PPC05; solid water phantom; scanning water tank
Central axis depth dose verification	*Purpose*: verification of spot energy and position and dose calculation by the TPS *Methods*: measure point dose at several depths (Fig. 2.9a)	MatriXX; PPC05; solid water phantom; scanning water tank
Relative 2D dose measurements	*Purpose*: 2D dose measurement at multiple depths allows detection of potentially large errors in spot lateral position as well as TPS dose modeling *Methods*: use 2D ion chamber array detector to measure three depths within the SOBP (proximal, middle, and distal). The γ-index was used for comparison of 2D dose distribution with a requirement of a 3% dose or 3-mm distance to agreement (Fig. 2.9b)	MatriXX; solid water phantom; (Fig. 2.10 is the example of 2D dose distribution comparison of RT and LT prostate fields)

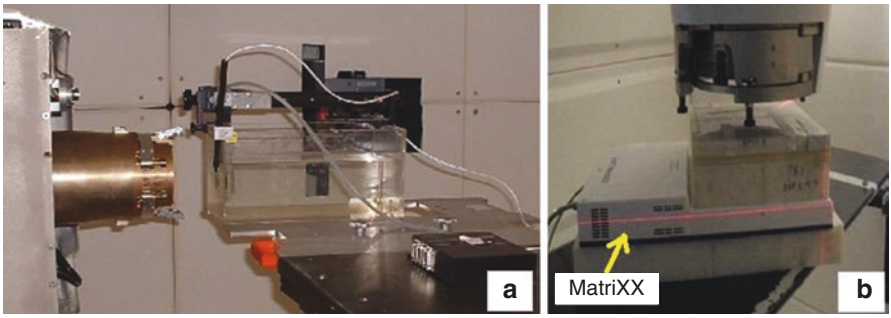

Fig. 2.9 (**a**) Rectangular water phantoms for depth dose measurements. (**b**) MatriXX 2D ion chamber array detector with plastic water phantoms

The average time based on this comprehensive PSQA procedure for each patient's plan was approximately 2 h for all three types of measurements and data analysis. For a busy center running 16-h treatment days and thus on average five new plans to start daily, it requires significant QA beam time after treatment and weekends. Therefore, it is highly desirable to simplify the procedure and improve the efficiency of PSQA. In most clinics today, measurements at the exact treatment gantry angle are not always performed due to the complicated workflow which requires a special couch mount device to hold heavy solid water and the MatriXX detector. Lomax et al. reported PSI's QA experiences using orthogonal dose profiles acquired by an ionization chamber array, typically at two different depths in water

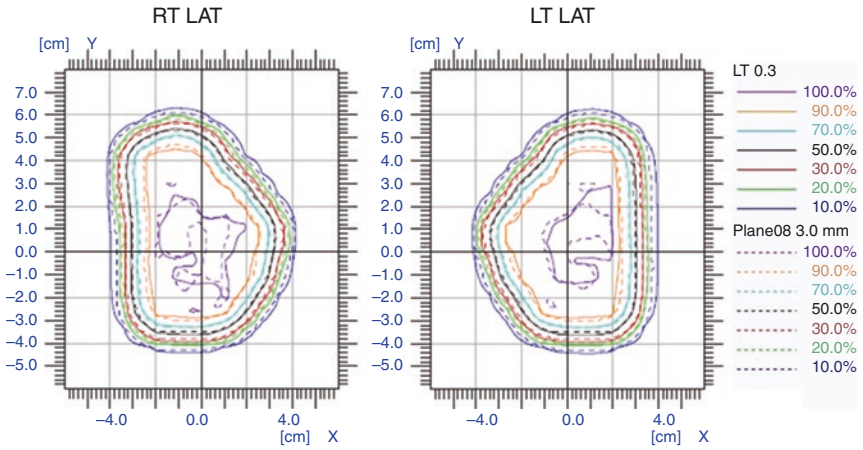

Fig. 2.10 Comparison of the two-dimensional dose distribution for a prostate proton SFUD plan at a depth of 23.4 cm. *Solid lines* indicate measurements obtained using MatriXX detector, and dashed lines indicate calculations obtained using the treatment planning system. (**a**) Right lateral field, (**b**) left lateral field

Fig. 2.11 Setup photo of DigiPhant with beam coming from the left (*red arrow*). The detector array automatically stops and acquires data at multiple programmed locations within the water tank during measurements (Permission pending IBA dosimetry)

[6]. Lin et al. [26] investigated the feasibility of using a waterproof housing to hold the MatriXX that is scanned in a water phantom (DigiPhant, IBA dosimetry) (Fig. 2.11). This new dosimetry tool could combine point dose, depth dose, and 2D dose distribution in one setup and significantly reduce the time and QA workload. Unfortunately such QA tools are not able to verify the gantry dependent parameters, e.g., current settings of all bending and steering magnets.

To further reduce the PSQA workload, Mackin et al. proposed a second-check dose calculation engine, HPlusQA. The study concluded that it could reduce the need for PSQA measurement by 64%. Zhu et al. [27] suggested incorporating both

independent dose calculation and treatment log file analysis to reduce the time required for measurements.

IMPT QA

IMPT is most often used in situations with complex patient anatomy and target, e.g., head and neck, CNS, and thoracic/GI. Compared to SFUD, each field in an IMPT plan is highly modulated in both energy and spot position. Although the principles of PSQA procedures are very similar to SFUD, they require more measurements and more detailed analysis. To the best of our knowledge, there is still no publication on comprehensive PSQA procedures for IMPT yet. In some institutions, IMPT field is normally measured in more different depths compared to SFUD. At MD Anderson, HPlusQA is implemented for IMPT PSQA as well.

Range Shifter Effects on PSQA for PBS

Range shifters (RS) are used often in PBS treatments for shallow targets, e.g., HNC and CNS. Beam modeling of RS is a separated option in some TPS. The QA result might be affected by the air gap and beam modeling. Initial result reported by Mackin et al. [17] suggested that the dose algorithm in certain planning system is accurately modeling the dose from the secondary radiation but not so for the effects on the distal falloff.

2.6.2.2 PSQA for Passive-Scattering

Passive-scattering beam delivery involves more hardware and system configurations compared to spot-scanning beam delivery, such as apertures, compensators, and the beam options with the specific scatterer settings, modulation wheels, etc. For each treatment field, apertures and compensators were manually checked; apertures must match with the treatment plan; compensator thickness tolerance is 0.5 mm (see Fig. 2.12). To make the process more quantitative and comprehensive, Yoon et al. [28]

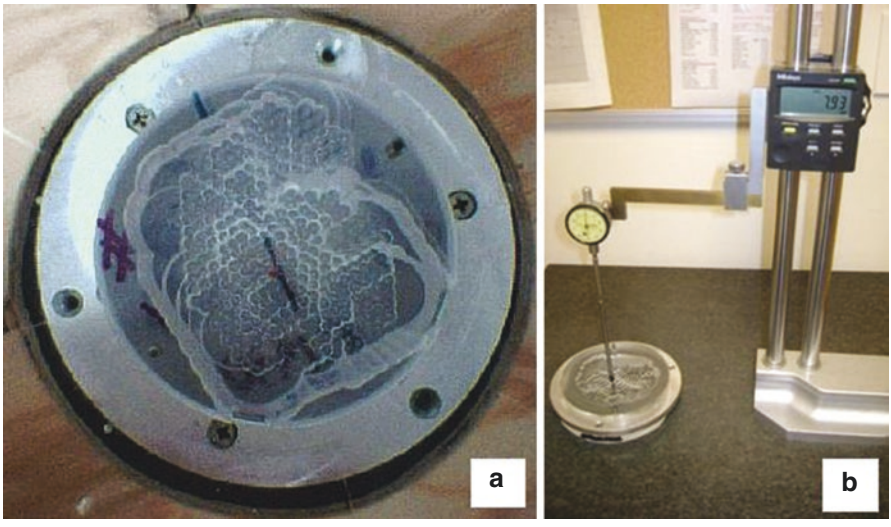

Fig. 2.12 (**a**) An example of an actual compensator used for proton beam treatment. (**b**) The device used to verify the thickness manually by measuring the height relative to the surface for a single-sided compensator

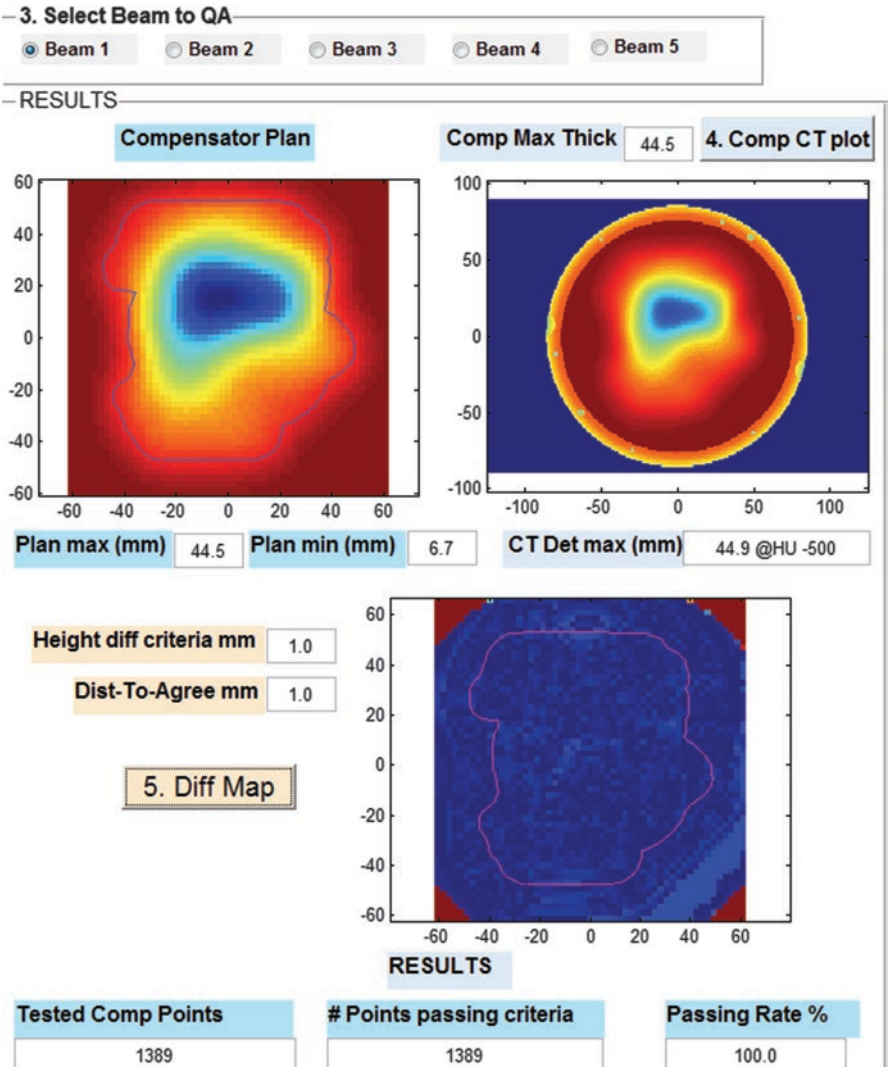

Fig. 2.13 User interface of an in-house developed compensator QA software based on CT image of the compensator at the Robert Wood Johnson Cancer Institute

suggested using CT to assess the quality of the compensator instead of the manual measurement. Figure 2.13 shows the workflow and user interface for the CT-based compensator QA method used at the Robert Wood Johnson Cancer Institute.

As described above, current TPS systems do not generally support the calculation of beam MU values for PS. The MUs are determined from measurements with ion chamber in water or water equivalent materials. Normally absolute dose is checked through measurement in the center of SOBP using a water tank or solid water combining with the PPC or ion chamber array. An analytic model based secondary check system is generally used.

2.7 Future Developments

Proton beam therapy technique has been advancing rapidly within this decade. Considering that PBS treatment technology became commercially available only less than 10 years ago [1], it is remarkable that nearly all new proton centers now are configured with a PBS only technique. However, treating moving targets remains the biggest challenge for PBS technique, owing to the interplay effects, as described above [6, 18, 20, 22–24]. A number of delivery techniques have been proposed to compensate the interplay effects by using, e.g., repainting [29], breath-holding [30], gating [31], and tracking [31]. Some of these techniques have been successfully implemented by certain vendors in some clinics. We are expecting more new techniques as well as more clinical data coming in the next decades to demonstrate the feasibility and value of treating moving tumors with PBS.

Another area with rapid improvement expected is image guidance for treatment, specifically the use of volumetric imaging. Although proton therapy once led the way to image guidance in radiotherapy by using orthogonal X-rays for patient setup from the very beginning, in recent years it fell behind conventional therapy where CBCT is now routinely used. The value of volumetric imaging has been recognized by the community of particle therapy now, and adoption of this technique has started. The first CBCT for proton system was just implemented commercially at the Roberts Proton Therapy Center at the University of Pennsylvania in 2015 which opens a new area of precise patient positioning and dose evaluation to improve treatment accuracy [32]. The use of in-room CT, or CT on rails, is another approach taken by certain vendors. Daily CT-/CBCT-based dose calculation and treatment adaptation should become a routine treatment option to further improve treatment outcomes [32].

Beam range uncertainties in patients have always been a major challenge to utilizing the full potential of the proton beam for target coverage and organ avoidance. Major efforts have been focused on increasing accuracy of the proton range calculation and delivery by using innovative imaging and detection devices such as prompt gamma camera [13], ultrasound detectors [33, 34], PET imaging [35], proton beam imaging [36] and the use of DECT [9]. Some of these new imaging techniques are expected to be clinical available soon. A prompt gamma camera system is currently in clinical testing at the University of Pennsylvania.

The technique of volumetric-modulated arc therapy (VMAT) has been widely used in photon therapy, with significantly shorter treatment time and possibly improved dose distribution when compared to standard intensity-modulated radiation therapy using static fields. It is a natural question if proton arc therapy can also improve dose distributions and robustness given the well-known issues of beam range uncertainty, anatomical variations, distal-end RBE uncertainties, limitations of spot sizes, etc. Exploration in this direction has started recently. Ding et al. proposed a novel spot-scanning proton arc (SPArc) algorithm to generate a robust, delivery-efficient and continuous proton arc plan, showing a promising dosimetric improvement over current IMPT technique especially in the reduction of integral dose and target conformity with comparable delivery time [37]. It is demonstrated for the first time that the concept of proton arc therapy could be clinical valuable and feasible through continuous delivery. Although implementing such treatment technique will need to overcome tough technical challenges, some of which may be more difficult than ever, efforts in this direction are expected to continue.

References

1. Smith A, Gillin M, Bues M, et al. The M. D. Anderson proton therapy system. Med Phys. 2009;36:4068–83.
2. Christopher G. Ainsley, James McDonough. Physics considerations in proton therapy. Radiation medicine rounds: proton therapy. C. Thomas and J. Metz (eds). Demos Medical Publishing LLC; New York: 2010.
3. Akagi T, Higashi A, Tsugami H, et al. Ridge filter design for proton therapy at Hyogo Ion Beam Medical Center. Phys Med Biol. 2003;48:N301–12.
4. Kooy HM, Schaefer M, Rosenthal S, et al. Monitor unit calculations for range-modulated spread-out Bragg peak fields. Phys Med Biol. 2003;48:2797–808.
5. Gillin MT, Sahoo N, Bues M, et al. Commissioning of the discrete spot scanning proton beam delivery system at the University of Texas M.D. Anderson Cancer Center, Proton Therapy Center, Houston. Med Phys. 2010;37:154–63.
6. Lomax AJ. Intensity modulated proton therapy and its sensitivity to treatment uncertainties 2: the potential effects of inter-fraction and inter-field motions. Phys Med Biol. 2008;53:1043–56.
7. Wang D, Dirksen B, Hyer DE, et al. Impact of spot size on plan quality of spot scanning proton radiosurgery for peripheral brain lesions. Med Phys. 2014;41:121705.
8. Ainsley CG, Yeager CM. Practical considerations in the calibration of CT scanners for proton therapy. J Appl Clin Med Phys. 2014;15:4721.
9. Hünemohr N, Paganetti H, Greilich S, et al. Tissue decomposition from dual energy CT data for MC based dose calculation in particle therapy. Med Phys. 2014;41:61714.
10. Xie Y, Yin L, Ainsley C, et al. TU-FG-BRB-01: dual energy CT proton stopping power ratio calibration and validation with animal tissues. Med Phys. 2016;43:3756.
11. Arbor N, Dauvergne D, Dedes G, et al. Monte Carlo comparison of x-ray and proton CT for range calculations of proton therapy beams. Phys Med Biol. 2015;60:7585–99.
12. España S, Paganetti H. The impact of uncertainties in the CT conversion algorithm when predicting proton beam ranges in patients from dose and PET-activity distributions. Phys Med Biol. 2010;55:7557–71.
13. Verburg JM, Riley K, Bortfeld T, et al. Energy- and time-resolved detection of prompt gamma-rays for proton range verification. Phys Med Biol. 2013;58:L37–49.
14. Kang Y, Zhang X, Chang JY, et al. 4D Proton treatment planning strategy for mobile lung tumors. Int J Radiat Oncol Biol Phys. 2007;67:906–14.
15. Richter D, Saito N, Chaudhri N, et al. Four-dimensional patient dose reconstruction for scanned ion beam therapy of moving liver tumors. Int J Radiat Oncol Biol Phys. 2014;89:175–81.
16. Hong TS, DeLaney TF, Mamon HJ, et al. A prospective feasibility study of respiratory-gated proton beam therapy for liver tumors. Pract Radiat Oncol. 2014;4:316–22.
17. Li Y, Kardar L, Li X, et al. On the interplay effects with proton scanning beams in stage III lung cancer. Med Phys. 2014;41:21721.
18. Grassberger C, Dowdell S, Lomax A, et al. Motion interplay as a function of patient parameters and spot size in spot scanning proton therapy for lung cancer. Int J Radiat Oncol Biol. Phys. 2013;86:380–6.
19. Dowdell S, Grassberger C, Paganetti H. Four-dimensional Monte Carlo simulations demonstrating how the extent of intensity-modulation impacts motion effects in proton therapy lung treatments. Med Phys. 2013;40:121713.
20. Zeng C, Plastaras JP, James P, et al. Proton pencil beam scanning for mediastinal lymphoma: treatment planning and robustness assessment. Acta Oncol Stockh Swed. 2016;55(9–10):1132–8.
21. Zeng C, Plastaras JP, Tochner ZA, et al. Proton pencil beam scanning for mediastinal lymphoma: the impact of interplay between target motion and beam scanning. Phys Med Biol. 2015;60:3013–29.
22. Rietzel E, Bert C. Respiratory motion management in particle therapy. Med Phys. 2010;37:449–60.
23. Li H, Zhu XR, Zhang X. Reducing dose uncertainty for spot-scanning proton beam therapy of moving Tumors by optimizing the spot delivery sequence. Int J Radiat Oncol Biol Phys. 2015;93:547–56.

24. Yu J, Zhang X, Liao L, et al. Motion-robust intensity-modulated proton therapy for distal esophageal cancer. Med Phys. 2016;43:1111–8.
25. Zhu XR, Poenisch F, Song X, et al. Patient-specific quality assurance for prostate cancer patients receiving spot scanning proton therapy using single-field uniform dose. Int J Radiat Oncol Biol Phys. 2011;81:552–9.
26. Lin L, Kang M, Solberg TD, et al. Use of a novel two-dimensional ionization chamber array for pencil beam scanning proton therapy beam quality assurance. J Appl Clin Med Phys. 2015;16:5323.
27. Zhu XR, Li Y, Mackin D, et al. Towards effective and efficient patient-specific quality assurance for spot scanning proton therapy. Cancers (Basel). 2015;7:631–47.
28. Yoon M, Kim J-S, Shin D, et al. Computerized tomography-based quality assurance tool for proton range compensators. Med Phys. 2008;35:3511–7.
29. Zenklusen SM, Pedroni E, Meer D. A study on repainting strategies for treating moderately moving targets with proton pencil beam scanning at the new Gantry 2 at PSI. Phys Med Biol. 2010;55:5103–21.
30. Mast ME, Vredeveld EJ, Credoe HM, et al. Whole breast proton irradiation for maximal reduction of heart dose in breast cancer patients. Breast Cancer Res Treat. 2014;148:33–9.
31. Shimizu S, Miyamoto N, Matsuura T, et al. A proton beam therapy system dedicated to spot-scanning increases accuracy with moving tumors by real-time imaging and gating and reduces equipment size. PLoS One. 2014;9:e94971.
32. Veiga C, Janssens G, Teng C-L, et al. First clinical investigation of CBCT and deformable registration for adaptive proton therapy of lung cancer. Int J Radiat Oncol Biol Phys. 2016;95:549–59.
33. Jones KC, Stappen FV, Bawiec CR, et al. Experimental observation of acoustic emissions generated by a pulsed proton beam from a hospital-based clinical cyclotron. Med Phys. 2015;42:7090–7.
34. Patch SK, Covo MK, Jackson A, et al. Thermoacoustic range verification using a clinical ultrasound array provides perfectly co-registered overlay of the Bragg peak onto an ultrasound image. Phys Med Biol. 2016;61:5621.
35. Zhu X, Fakhri GE. Proton therapy verification with PET imaging. Theranostics. 2013;3:731–40.
36. Bentefour EH, Schnuerer R, Lu H-M. Concept of proton radiography using energy resolved dose measurement. Phys Med Biol. 2016;61:N386.
37. Ding X, Li X, Zhang JM, et al. Spot-scanning proton arc (SPArc) therapy—the first robust and delivery-efficient spot-scanning arc therapy. Int J Radiat Oncol Biol Phys. 2016;96(5):1107–16.